# Mechanical Properties and Strengthening Mechanism of Pure Ti Powder Composite Material Reinforced with Carbon Nano Particles†

**MIMOTO Takanori*, NAKANISHI Nozomi*, UMEDA Junko** and KONDOH Katsuyoshi*****

**Abstract**

*The strengthening mechanisms of titanium-carbon black (CB) nano particle composite materials were investigated quantitatively in the present study. The titanium matrix composite (TMC) specimens were prepared via a powder metallurgy (P/M) route including the wet coating process for composite titanium (Ti) powders with un-bundled CB nano particles, consolidation by spark plasma sintering (SPS) and subsequent hot extrusion. The extruded TMC, with carbon content of 2.66 at.%, exhibited excellent tensile strength of 837 MPa in 0.2%YS, 899 MPa in UTS and 18.7% in elongation at ambient temperature. In this composite, some of additive CB nano particles were dissolved into the Ti matrix as a solid solution element. The other CBs and Ti matrix were chemically reacted when sintering, and resulted in the in-situ formed titanium carbide (TiC) compounds, which were uniformly distributed throughout the Ti matrix. These TiC dispersoids promoted the dynamic recrystallization during hot extrusion process, and resulted in the Ti grain refinement. Consequently, carbon solid solution hardening, TiC dispersion strengthening and grain refinement enhanced the mechanical performance of the TMC. In particular, the effect of TiC reinforcements, accounting for about 60% of the whole strengthening behavior, played the most significant role.*

**KEY WORDS: (Titanium matrix composite), (Carbon black particles), (Tensile properties), (Solid solution hardening), (Dispersion strengthening), (*In-situ* formed titanium carbide)**

## 1. Introduction

Titanium materials have recently attracted considerable interests as industrial materials because of their excellent characteristics such as low density, high specific strength and superior corrosion resistance. Ti-6Al-4V alloy, having a remarkable mechanical strength, is one of the most popular Ti alloys. They are widely used in various industrial applications, for example, automotive, surgical implants and marine applications[1, 2]. In particular, they are quite important to reduce the weight of aircraft components from a view point of both $CO_2$ emission reduction and fuel efficiency improvement[3]. Moreover, they are free from an electrochemically galvanic corrosion between carbon composite, such as carbon fiber reinforced plastics (CFRP). Accordingly, Ti materials are very suitable for aircraft applications, especially the advanced aircrafts using a large amount of carbon composites, for example, the newest of Airbus A380 and Boeing 787. On the other hand, the expensive Ti alloy products, resulting from the use of rare earths like vanadium as the alloying elements and their poor formability, prevent their applications from extensive spreading. From a standpoint of these contexts, a cost-effective Ti material with high mechanical performance is strongly required. In the previous research, un-alloyed pure Ti powder for a matrix powder and CB nano particles for a reinforcing element were employed as promising low cost starting materials[4, 5]. The most remarkable feature in that study was that CB nano particles were extremely cheap because they were collected from wasted black ink cartridges from inkjet printing. The Ti-CB nano particles powder composite materials showed equal or greater tensile properties than those of conventional Ti-6Al-4V as cast material. This result specifically indicates the usefulness of cheap CB particles as a reinforcing element and the fabrication approach for cost-effective high strength Ti materials. Moreover, those TMCs could be expected to overcome the high cost problem, the biggest challenge for high strength Ti materials. However, the strengthening mechanism and the correlation between microstructural and mechanical properties were not investigated in detail.

† Received on December 26, 2011
* Graduate Student
** Assistant Professor
*** Professor

Transactions of JWRI is published by Joining and Welding Research Institute, Osaka University, Ibaraki, Osaka 567-0047, Japan

The understanding of strengthening mechanisms is quite important to control the material performance. Moreover, the materials with tailor-made properties are effective for the cost reduction from the view point of manufacturing process. In the present study, the Ti-CB nano particles powder composite materials were fabricated via P/M route, involving wet coating process, SPS consolidation process and hot extrusion process. The microstructural analysis and mechanical properties evaluation for the extruded composites were carried out. The correlation between microstructures and mechanical responses was discussed in detail, and the strengthening mechanisms were clarified by both theoretical approaches and the above investigation results.

## 2. Experimental

Pure Ti powder (TOHOTEC, TC-450) shown in **Fig. 1** (a), having a median particle size of 21.9 μm, was employed as a starting material in this study. The impurity compositions of the starting powder were as follows; Fe: 0.03, Si: 0.01, Mg: <0.001, Cl: 0.002, O: 0.21, N: 0.009, C: 0.014 (in mass%). CB nano particles shown in **Fig. 1** (b), the other starting material, were uniformly dispersed in black ink which collected from used black ink cartridges from inkjet printing. The particle size, evaluated with laser scattering particle size distribution analyzer (HORIBA, LA-950), was 86 nm in median diameter. Dilute black ink solutions with various CB contents were produced by adding pure water. These dilute solutions were served to a wet coating process. Starting pure Ti powder was immersed into the solution in the wet process, and subsequently dried in an oven (Yamato Scientific Co., Ltd., DX301) at 373 K for 10.8 ks. On the dried powder surface, not only CB particles but also organic constituents originating from the black ink remained. The organic constituents should be removed before consolidation because they would otherwise convert to gases during consolidation process, and result in impeding metallurgical bonding and pore defects in consolidated samples. In order to thermally decompose the residual organic constituents, the dried powder was heated in a horizontal tube furnace (Asahi rika, ARF-2-500) at 873 K for 3.6 ks in argon (Ar) gas atmosphere. The heat treatment temperature was optimized by the results of thermogravimetric analysis for black ink using TG-DTA (SHIMADZU, DTG-60). After the thermal removal of the organic constituents, the Ti-CB composite powder was consolidated into a billet of 42 mm diameter via an SPS (SPS Syntex Inc., SPS-1030S) process[6] at 1073 K for 1.8 ks with 30 MPa pressure in vacuum. The SPSed billet was heated to 1273 K and kept for 180 s under Ar gas atmosphere. The preheated billet was then immediately served to hot extrusion process using a hydraulic direct press machine (Shibayamakikai Co., SHP-200-450) with a press capacity of 2000 kN. The extrusion ratio and speed were 37.7 and 3.0 mm/s, respectively. The mold and die temperature was 673 K. The extruded rods were of 7 mm in diameter and approximately 600 mm in length. Carbon, oxygen and nitrogen contents of the extruded composites were measured by carbon/sulfur determinator (LECO Co., CS-200) and nitrogen/oxygen determinator (LECO Co., TC-300), respectively. The microstructures and phase characterization of the extruded specimens were evaluated with optical microscope (OM, OLYMPUS, BX-51P), field emission scanning electron microscope (FE-SEM, JEOL, JSM-6500F) with energy dispersive X-ray spectrometer (EDS, JEOL, JED-2300) and X-ray diffraction (XRD, SHIMADZU, XRD-6100). In the sample preparation, the extruded composites were sectioned parallel to the extrusion direction, abraded with #240 ~ #4000 SiC abrasive papers, and then, buffed with 0.3 μm and 0.05 μm $Al_2O_3$ particle. After each step, specimen surfaces were carefully rinsed in ethanol with ultrasonic vibration. The electron back-scattered diffraction (EBSD) texture measurements were carried out by using FE-SEM equipped with a TSL EBSD orientation imaging system. The Kikuchi patterns[7] were obtained with an ultra-sensitive CCD camera and processed with TSL OIM Data Collection 5.31 and TSL OIM Analysis 5.31 software from TSL Solutions K.K. For EBSD analysis, the buffed samples were electrochemically finished with the electro-polishing solution consisting of 95% $CH_3COOH$ + 5% $HClO_4$ at the voltage of 50 V for 90 s.

The extruded rods were machined into tensile test specimens of 3.0 mm diameter and 20 mm gauge length. The ambient tensile properties were evaluated using a universal testing machine (SHIMADZU, AUTOGRAPH AG-X 50kN) under a strain rate of $5.0\times10^{-4}$ /s. The hardness tests were conducted with a Vickers microhardness tester (SHIMADZU, HMV-2T) with loading weight of 1.961 N for 15 s. The Young's moduli were measured with a Young's modulus measurement device using resonant frequency technique (Nihon Techno-Plus Corp., JE-RT).

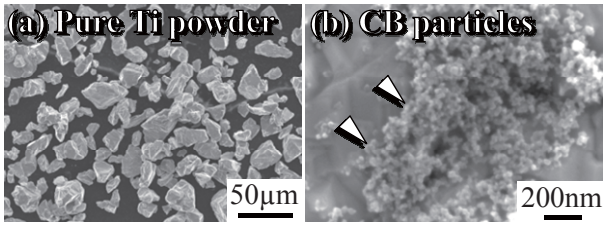


**Fig. 1** Morphologies of pure Ti powder (a) and carbon black nano particles (b), employed as stating materials in this experiment.

## 3. Results and Discussion

### 3.1 Microstructural analysis on extruded Ti-CB composite materials

In the present study, 7 extruded composite materials with various carbon contents (COMP1-7) were prepared. Carbon, oxygen and nitrogen contents of each specimen are summarized in **Table 1**.

Optical microstructures and grain distribution by EBSD analysis of COMP1 (a), 4 (b), 5 (c), 7 (d)

specimens are shown in **Fig. 2**. The average grain sizes of Ti matrix are also shown in the figure. All specimens consisted of equiaxed $\alpha$-Ti phase as a matrix. In addition, *in-situ* formed dispersoids were uniformly distributed throughout the matrix in COMP5 and 7 specimens, and the amount of the dispersoids increased in proportion to the additive carbon content. XRD analysis results of these specimens, presented in **Fig. 3**, clearly indicated the dispersoids were titanium carbide (TiC) compounds. This is consistent with not only the above observation results but also EDS analysis on the dispersoids. In addition, the standard free energy change ($\Delta G^{o}$) of TiC formation is −172 kJ/mol at 1073 K[8], which also ensures that the *in-situ* TiC formation in sintering process is possible. The TiC particles promoted both dynamic recrystallization during the hot extrusion process and pinning effect during grain growth, which led to a grain refinement especially in COMP7 specimen with a great quantity of TiC particles as shown in **Fig. 2** (d). Furthermore, COMP7 specimen had a randomized texture compared with other specimens, indicating the dynamic recrystallization[9]. On the other hand, COMP1 and 4 specimens contained no TiC dispersoid as shown in **Fig. 2** (a) and (b). This is certainly related to the carbon solubility limit for $\alpha$-Ti matrix of about 0.2 at.%[10, 11], and additive carbon in these specimens was dissolved into an hcp lattice of $\alpha$-Ti, especially c axis. This was confirmed with the relationship between lattice constant of c axis and carbon content shown in **Fig. 4**, calculated from the peak shift in XRD results. The increasing rate of these plots was 0.0145 Å/at.%, which substantially accords with that in previous report (0.0127 Å/at.%[12]). Consequently, the carbon added to COMP1-4 specimens was completely dissolved into $\alpha$-Ti matrix, and TiC compounds were synthesized in COMP5-7 specimens with the carbon concentration over solubility limit.

**Table 1** Compositions of carbon, oxygen and nitrogen impurities of COMP1-7 specimens.

| | Carbon | | Oxygen | Nitrogen |
|---|---|---|---|---|
| | (mass%) | (at.%) | (mass%) | (mass%) |
| COMP1 | 0.017 | 0.065 | 0.37 | 0.024 |
| COMP2 | 0.025 | 0.096 | 0.32 | 0.015 |
| COMP3 | 0.036 | 0.138 | 0.35 | 0.013 |
| COMP4 | 0.065 | 0.250 | 0.35 | 0.017 |
| COMP5 | 0.154 | 0.590 | 0.34 | 0.017 |
| COMP6 | 0.433 | 1.645 | 0.41 | 0.019 |
| COMP7 | 0.707 | 2.662 | 0.46 | 0.018 |

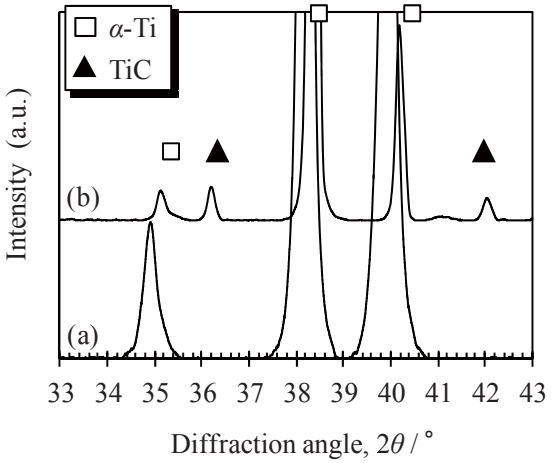


**Fig. 3** XRD profiles of COMP4 specimen (a) without *in-situ* formed dispersoids and COMP7 specimen (b) with TiC dispersoids.

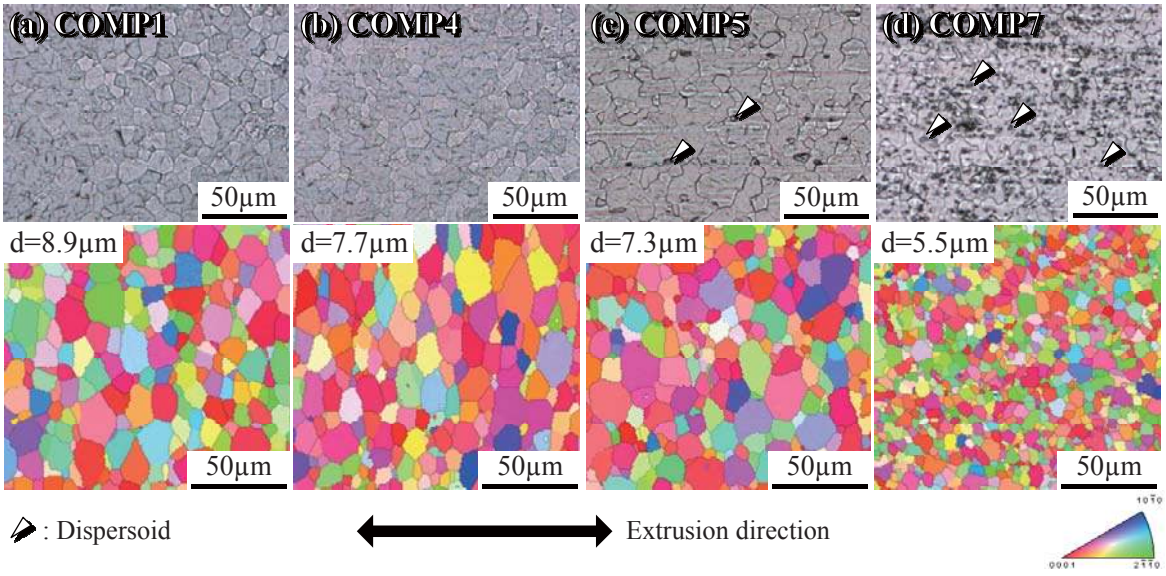


**Fig. 2** Optical microstructures and grain distributions captured by EBSD of COMP1 (a), COMP4 (b), COMP5 (c) and COMP7 (d) specimens.

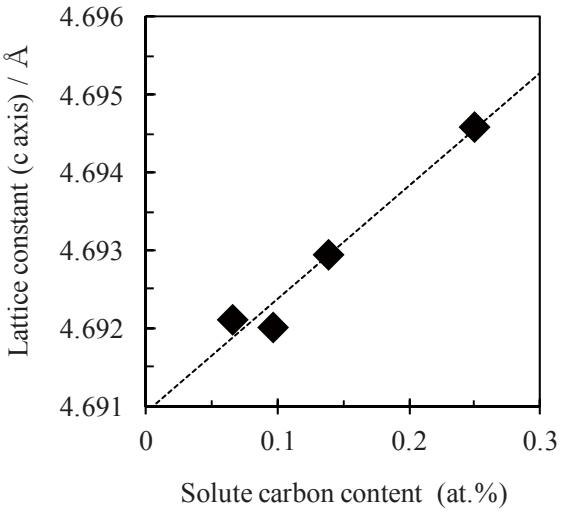


**Fig. 4** Relationship between lattice constant (c axis) of $\alpha$-Ti matrix and solute carbon content of COMP1-4 specimens.

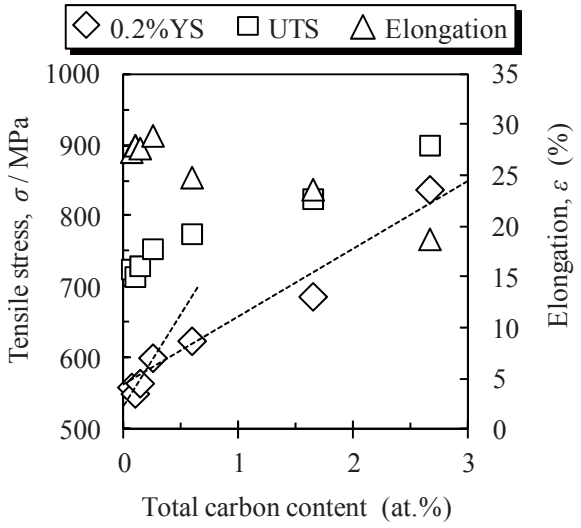


**Fig. 5** Dependence of ambient tensile properties of COMP1-7 specimens on total carbon content.

### 3.2 Mechanical behavior and strengthening mechanism of extruded Ti-CB composite materials

Ambient tensile properties of COMP1-7 specimens are summarized in **Fig. 5**. The tensile strength was significantly increased with higher carbon content. In particular, COMP7 with the highest carbon content exhibited 0.2%YS of 837 MPa, UTS of 899 MPa and elongation of 18.7%, which are comparable to those of conventional Ti-6Al-4V alloy[1]. Furthermore, there is a large difference between 0.2%YS increasing rate of COMP1-4 (257 MPa/at.%[C]) and that of COMP4-7 (95 MPa/at.%[C]). The results of hardness test exhibited the same trend as tensile properties depending on total carbon content as shown in **Fig. 6** (COMP1-4: 101 (Hv)/at.%[C], COMP4-7: 24 (Hv)/at.%[C]). These suggest the change of main strengthening mechanism in COMP1-4 and COMP4-7 specimens. On the basis of the microstructural analysis, the mechanical strength of COMP1-4 and COMP4-7 specimens could be enhanced by solid solution hardening by solute carbon atoms and TiC reinforcements dispersion strengthening, expressed by rule of mixture, respectively.

First, the theoretical values of carbon solid solution hardening in COMP1-4 specimens were estimated from Friedel-Fleischer (F-F) model[12, 13] in order to compare experimental values with theoretical values. In addition, strengthening effects on 0.2%YS were evaluated relatively by using COMP1 specimen as a basis here. Solute atoms, dissolved into metal matrix, have an elastic interaction with moving dislocations, as schematically illustrated in **Fig. 7** (a). The F-F model gives the breakthrough stress, to release dislocation from a solute atom as obstacle, as following equation (1), which yields the 0.2%YS increment ($\Delta\sigma_y$) depending on the atomic concentration of solute element ($c$).

$$\Delta\sigma_y = \frac{\tau_0}{S_F} = \frac{F_m^{3/2}}{S_F b^2}\sqrt{\frac{c}{2E_L}} \qquad (1)$$

In the above equation, $\tau_0$, $S_F$, $F_m$, $b$ and $E_L$ are critical resolved shear stress, Schmid factor, maximum interaction force between a solute atom and a dislocation, Burgers vector and dislocation line tension, respectively. The comparison between theoretical calculation of equation (1) and experimental results are presented in **Fig. 7** (b). In addition, other strengthening effects, grain refinement and oxygen solid solution, on strength increment were removed from original experimental data so as to obtain the 0.2%YS increment only by carbon solid solution hardening[14, 15]. The calculation results gave good fitting to the revised experimental data, which indicates that the carbon solid solution hardening surely improved the mechanical strength of COMP1-4 specimens.

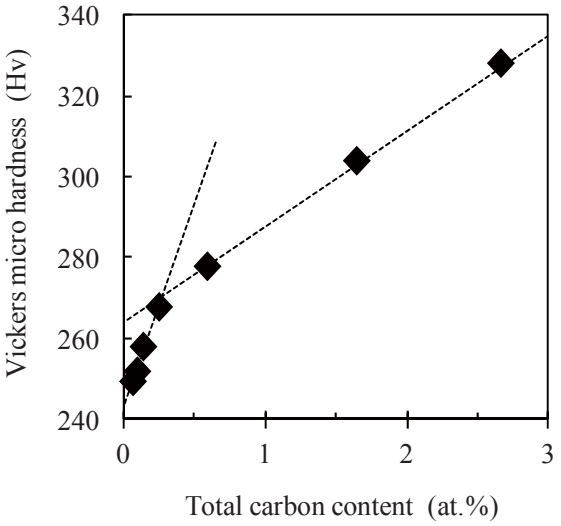


**Fig. 6** Dependence of Vickers micro hardness of COMP1-7 specimens on total carbon content.

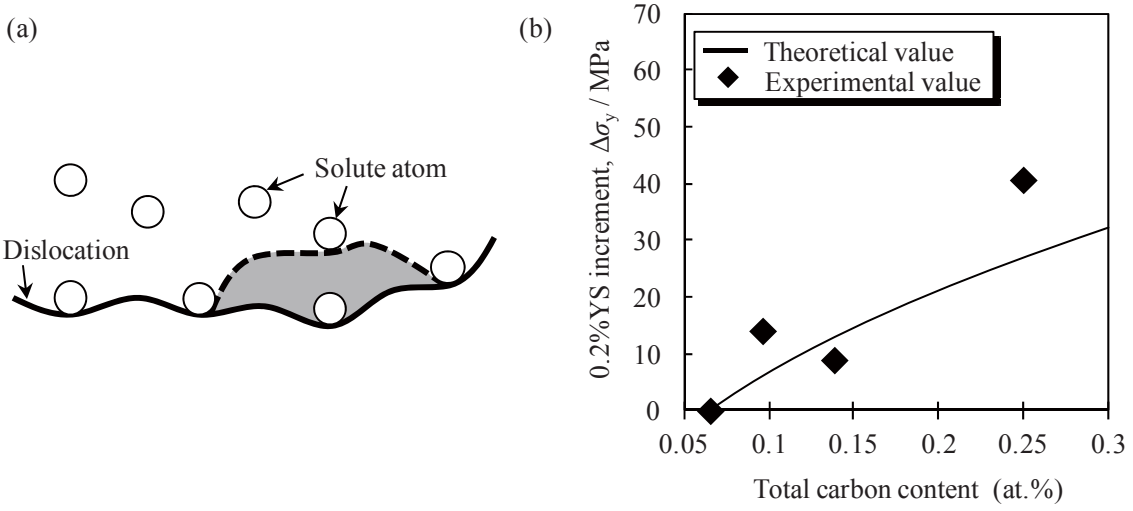


**Fig. 7** Schematic model of solid solution hardening (a) and comparison of theoretical and experimental values of 0.2%YS increment of COMP1-4 specimens (b).

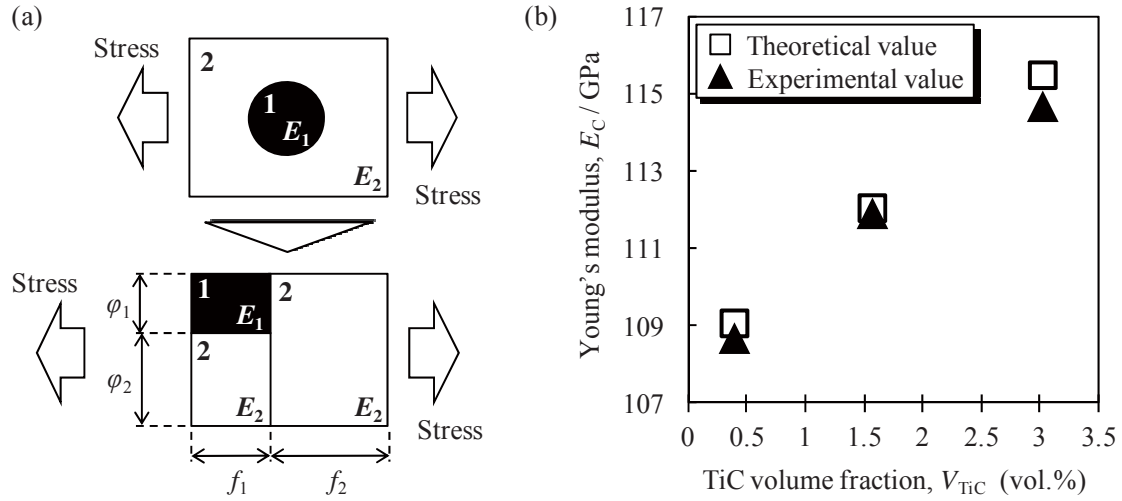


**Fig. 8** Schematic model of rule of mixture for particulate-reinforced composite (a) and comparison of theoretical and experimental values of Young's modulus of COMP5-7 specimens (b).

Many reports show that reinforcing dispersoids, such as TiC and TiB, enhance not only tensile strength but also Young's modulus[16-21]. In the present study, COMP5 with 0.39, COMP6 with 1.57 and COMP7 with 3.02 vol.% *in-situ* formed TiC particles exhibited Young's modulus of 109, 112 and 115 GPa, respectively, compared to 108 GPa of COMP4 with no TiC dispersoids. The improvement of Young's modulus was certainly related to the incremental strength of those specimens. Young's modulus can be estimated from the theoretical model, which is the rule of mixture for particulate-reinforced composite[22], described in **Fig. 8** (a). Area 1 (black area) and area 2 (white area) indicate reinforcing phase and matrix phase, respectively. The theoretical Young's modulus ($E_C$) was calculated by the following equation (2).

$$E_C = \left( \frac{f_1}{\varphi_1 E_1 + \varphi_2 E_2} + \frac{f_2}{E_2} \right)^{-1} \qquad (2)$$

$E_1$ and $E_2$ are Young's modulus of reinforcing phase (TiC: 450 GPa[23]) and matrix phase (COMP4: 108 GPa). $f_1$, $f_2$, $\varphi_1$ and $\varphi_2$ exhibit the length ratio ($f_1 + f_2 = 1$, $\varphi_1 + \varphi_2 = 1$) as illustrated in **Fig. 8** (a). The experimental and theoretically predicted values for Young's modulus of COMP5-7 specimens are shown in **Fig. 8** (b). The experimental results were found to be in excellent agreement with the theoretical calculation by the equation (2). The results indicate that the *in-situ* formed TiC reinforcements principally improve the mechanical properties of COMP5-7 specimens, and also suggest the possibility of a tailor-made composite material with controllable properties. The excellent agreement between experimental and theoretical values was probably due to the high interfacial strength between TiC reinforcements and Ti matrix, which was enough to effectively transfer tensile loading from matrix to reinforcements.

In addition to the above two strengthening behavior, grain refinement effect also contributed to the increase in the mechanical strength of each specimen as mentioned in

**Fig. 2**. Consequently, these results are summarized in **Fig. 9**. This obviously shows that the strength increment of COMP1-4 and COMP4-7 are chiefly due to solid solution hardening by solute carbon atoms and dispersion strengthening by *in-situ* formed TiC reinforcing particles with adequate interfacial strength between Ti matrix, summarized in the rule of mixture, respectively. The carbon, both solute element and element of TiC compounds, was originated from additive CB nano particles.

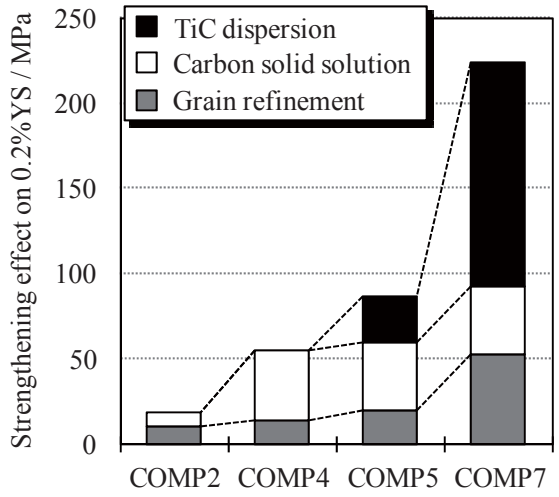


**Fig. 9** Strengthening effects on 0.2%YS by each mechanism in COMP2, 4, 5, 7 specimens.

## 4. Conclusions

In this study, microstructures, mechanical properties and strengthening mechanism of P/M Ti-CB nano particles composite materials were investigated in detail. The Ti-CB composites principally consisted of equiaxed $\alpha$-Ti phase with completely dissolved carbon, and in addition to the matrix phase, some composites, with high carbon concentration over carbon solubility limit, contained *in-situ* formed TiC dispersoids as a reinforcing phase. The composite, with the highest carbon concentration in this study, exhibited superior tensile properties of 837 MPa in 0.2%YS, 899 MPa in UTS and 18.7% in elongation, compared to a conventional Ti-6Al-4V alloy. The enhanced mechanical performance in this composite material was due to grain refinement (23%), solid solution hardening by solute carbon atoms (18%) and especially dispersion strengthening by TiC reinforcements (58%). These results suggested the possibility of tailor-made Ti-CB composite material which satisfied various mechanical requirements.

## Acknowledgement

A part of this study was financially supported by a grant for research and technology development on waste management, Ministry of the Environment, government of Japan.

## References

1) R. Boyer, E.W. Collings, and G. Welsch, eds., *Materials Properties Handbook: Titanium Alloys*, (1994) 165-245.
2) C. Leyens and M. Peters, eds., *Titanium and Titanium Alloys: Fundamentals and Applications*, (2003) 20-21.
3) J.C. Williams and E.A. Starke, Jr., *Acta Materialia*, 51 (2003) 5775-5799.
4) T. Threrujirapapong, K. Kondoh, H. Imai, J. Umeda, and B. Fugetsu, *Materials Transactions*, 50 (12) (2009) 2757-2762.
5) T. Mimoto, N. Nakanishi, T. Threrujirapapong, J. Umeda, and K. Kondoh, *MS&T'11 – Materials Science and Technology 2011 Conference & Exhibition*, (2011) 1002-1009.
6) E.A. Olevsky, S. Kandukuri, and L. Froyen, *Journal of Applied Physics*, 102 (114913) (2007).
7) D.G. Coates, *Philosophical Magazine*, 16 (1967) 1179-1184.
8) I. Barin, F. Sauert, E. Schultze-Rhonhof, and W.S. Sheng, *Thermochemical Data of Pure Substances, Part II*, (1989) 1528.
9) K.K. Denga, K. Wua, X.J. Wanga, Y.W. Wua, X.S. Hua, M.Y. Zhenga, W.M. Ganb, and H.G. Brokmeierb, *Materials Science and Engineering A*, 527 (2010) 1630-1635.
10) H. Nishimura and H. Kimura, *Nippon Kinzoku Gakkaishi*, 20 (1956) 524-528.
11) R.L. Bickerdike and G. Hughes, *Journal of the Less-Common Metals*, 1 (1959) 42-49.
12) H. Conrad, *Progress in Materials Science*, 26 (1981) 123-403.
13) R.W. Cahn, *Physical Metallurgy Fourth, revised and enhanced edition Volume III*, (1996) 2018-2019.
14) Y. Kobayashi, Y. Tanaka, K. Matsuoka, K. Kinoshita, Y. Miyamoto, and H. Murata, *Journal of the Society of Materials Science*, 54 (1) (2005) 65-72.
15) T. Yoshimura, T. Threrujirapapong, H. Imai, and K. Kondoh, *The 7th Pacific Rim International Conference on Advanced Materials and Processing*, (2010).
16) H.T. Tsang, C.G. Chao, and C.Y. Ma, *Scripta Materialie*, 37 (9) (1997) 1359-1365.
17) W.J. Lu, D. Zhang, X.N. Zhang, R.J. Wu, T. Sakata, and H. Mori, *Materials Science and Engineering A*, 311 (2001) 142-150.
18) R. Angers, M.R. Krishnadev, R. Tremblay, J.-F. Corriveau, and D. Dub´e, *Materials Science and Engineering A*, 262 (1999) 9-15.
19) S. Ranganath, M. Vijayakumar, and J. Subrahmanyam, *Materials Science and Engineering A*, 149 (1992) 253-257.
20) D.R. Ni, L. Geng, J. Zhang, and Z.Z. Zheng, *Materials Science and Engineering A*, 478 (2008) 291-296.
21) S.C. Tjong and Yiu-Wing Mai, *Composites Science and Technology*, 68 (2008) 583-601.
22) JSMS, *Engineering Materials*, (2009) 338-361.
23) D. Vallauri, I.C. At´ıas Adri´an, and A. Chrysanthou, *Journal of the European Ceramic Society*, 28 (2008) 1697-1713.